THE JOURNAL OF BIOLOGICAL CHEMISTRY VOL. 286, NO. 19, pp. 16783–16789, May 13, 2011
© 2011 by The American Society for Biochemistry and Molecular Biology, Inc. Printed in the U.S.A.

Structural Study of the Complex Stereoselectivity of Human Butyrylcholinesterase for the Neurotoxic V-agents*

Received for publication, December 6, 2010, and in revised form, February 28, 2011 Published, JBC Papers in Press, March 23, 2011, DOI 10.1074/jbc.M110.209569

Marielle Wandhammer[‡§], Eugénie Carletti[‡], Marcel Van der Schans[¶], Emilie Gillon[‡], Yvain Nicolet[‖], Patrick Masson[‡], Maurice Goeldner[§], Daan Noort[¶], and Florian Nachon[‡1]

From the [‡]Département de Toxicologie, Institut de Recherche Biomédicale des Armées-CRSSA, 38700 La Tronche, France, the [§]Laboratoire de Conception et Application de Molécules Bioactives, UMR 7199, Faculté de Pharmacie, 67400 Illkirch, France, the [¶]Research Group Diagnosis and Therapy, Business Unit Biological and Chemical Protection, TNO Defence, Security and Safety, 2288 GJ Rijswijk, The Netherlands, and the [‖]Laboratoire de Cristallographie et Cristallogenèse des Protéines, Institut de Biologie Structurale, 38027 Grenoble, France

Nerve agents are chiral organophosphate compounds (OPs) that exert their acute toxicity by phosphorylating the catalytic serine of acetylcholinesterase (AChE). The inhibited cholinesterases can be reactivated using oximes, but a spontaneous time-dependent process called aging alters the adduct, leading to resistance toward oxime reactivation. Human butyrylcholinesterase (BChE) functions as a bioscavenger, protecting the cholinergic system against OPs. The stereoselectivity of BChE is an important parameter for its efficiency at scavenging the most toxic OPs enantiomer for AChE. Crystals of BChE inhibited in solution or *in cristallo* with racemic V-agents (VX, Russian VX, and Chinese VX) systematically show the formation of the P_S adduct. In this configuration, no catalysis of aging seems possible as confirmed by the three-dimensional structures of the three conjugates incubated over a period exceeding a week. Crystals of BChE soaked in optically pure VX_R-(+) and VX_S-(−) solutions lead to the formation of the P_S and P_R adduct, respectively. These structural data support an in-line phosphonylation mechanism. Additionally, they show that BChE reacts with VX_R-(+) in the presence of racemic mixture of V-agents, at odds with earlier kinetic results showing a moderate higher inhibition rate for VX_S-(−). These combined results suggest that the simultaneous presence of both enantiomers alters the enzyme stereoselectivity. In summary, the three-dimensional data show that BChE reacts preferentially with P_R enantiomer of V-agents and does not age, in complete contrast to AChE, which is selectively inhibited by the P_S enantiomer and ages.

The acute toxicity of organophosphorus nerve agents (OPs)[2] is due to rapid phosphorylation of acetylcholinesterase (AChE; EC 3.1.1.7) at the neuronal synapses and neuromuscular junctions (1, 2). What follows is an accumulation of acetylcholine that leads, among other cholinergic symptoms, to respiratory failure and even death. One strategy to prevent AChE inhibition is to scavenge the nerve agent before it can reach its synaptic target. Butyrylcholinesterase (BChE; EC 3.1.1.8), abundant in human (3), functions as a natural bioscavenger of nerve agents (4, 5). A large amount of BChE injected intravenously or intramuscularly scavenges the nerve agents and protect animals against 3–5 LD_{50} of soman and VX (6). BChE purified from human plasma (Baxter Healthcare Corporation) is one enzyme source. This product is under consideration for its development as a stoichiometric bioscavenger for pretreatment of OP intoxication.

The catalytic serine of cholinesterases is located at the bottom of a gorge, surrounded by pockets, named from the part of the native substrate they bind. In AChE, the acyl-binding pocket is much smaller than the choline-binding pocket. Therefore, AChE exerts a strong enantioselectivity on chiral OPs, bearing substituents of different sizes. For example, hAChE reacts about 5×10^4 times more rapidly with P_S diastereoisomers of soman because the large pinacolyl and small methyl substituents fit, respectively, in the choline-binding pocket and acyl-binding pocket (7). The acyl-binding pocket of BChE is much wider than that of AChE and is therefore expected to be less selective for some OPs. This is important in regard to the amount of enzyme required to scavenge one equivalent of racemic nerve agent. Indeed, half an equivalent of BChE is sufficient if the enzyme binds preferably the same enantiomer as AChE. At least one equivalent is necessary if BChE binds equally both enantiomers or preferably the less toxic enantiomer.

Several lines of evidence suggest that BChE and hAChE have a different stereoselectivity for V-agents: VX, Russian VX (VR), and Chinese VX (CVX) (Scheme 1). One piece of evidence comes from a spontaneous time-dependent dealkylation of the V-agent adduct of cholinesterases, called aging, which leads to a resistance toward oxime reactivation (8). The dealkylation mechanism for alkoxy-OP adducts is stereoselective because it involves residues located in the choline-binding pocket of BChE. Accordingly, no aging will occur if the alkoxy substituent of V-agents is not pointing toward this pocket. A marginal aging rate is reported for VX-inhibited BChE ($t_{1/2}$ = 77 h), and

* This work was supported by Direction Générale de l'Armement under Programme d'Etude Amont Grants 08co501, ANR-06-BLAN-0163, and ANR-09-BLAN-0192 (to F. N.) and Defense Threat Reduction Agency Grant CBDIF07-THER01-2-0038 (to D. N., F. N., and M. G.).

The atomic coordinates and structure factors (codes 2XQF, 2XQG, 2XQI, 2XQJ, and 2XQK) have been deposited in the Protein Data Bank, Research Collaboratory for Structural Bioinformatics, Rutgers University, New Brunswick, NJ (http://www.rcsb.org/).

[1] To whom correspondence should be addressed: Département de Toxicologie, Institut de Recherche Biomédicale des Armées-CRSSA, 24 av. des Maquis du Grésivaudan, 38700 La Tronche, France. Fax: 205-934-7437; E-mail: florian@nachon.net.

[2] The abbreviations used are: OP, organophosphate; AChE, acetylcholinesterase; BChE, butyrylcholinesterase; CVX, Chinese VX; h, human; PDB, Protein Data Bank; VR, Russian VX; TLS, translation libration screw motion.

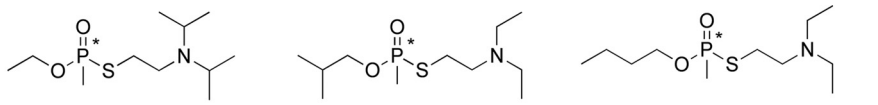

Diisopropylamino-ethyl-O-ethyl methylphosphonothioate (VX)

Diethylamino-ethyl-O-isobutyl methylphosphonothioate (VR)

Diethylamino-ethyl-O-butyl methylphosphonothioate (CVX)

SCHEME 1. **Chemical structures of V-agents, VX, VR, and CVX.**

no aging could be detected for VR-inhibited BChE (9). Furthermore, mass spectrometry analysis shows that no aged adduct was detectable for BChE treated with an excess solution of racemic VX or VR (10). This suggests that for these adducts, the alkoxy substituent is usually not located in the choline-binding pocket. This contrasts with the view offered by the x-ray structure of *Torpedo californica* AChE inhibited by VX with the ethoxy substituent located in the choline-binding pocket and able to age (11). This leads to the conclusion that BChE and AChE have opposite stereoselectivity.

However, measurements of the inhibition rate of separated VX isomers by independent laboratory showed that VX_S-(−) inhibits BChE a few-fold faster than VX_R-(+), whereas the difference in rate is more than 2 orders of magnitude for hAChE (12, 13). This in turn leads to the conclusion that both cholinesterases share the same stereoselectivity for VX_S-(−) but that AChE is much more stereoselective than BChE. This is consistent with recent *in vivo* experiment showing that a molar equivalent of BChE is required to protect against racemic VX (14).

Interestingly, these early results puzzlingly suggest that the stereoselectivity of BChE differs when exposed to racemic or optically pure solutions of VX. In this structural study, we investigate, at the molecular level, which enantiomer of VX, VR, and CVX reacts preferentially with BChE. We determine the inhibition mechanism for both enantiomers of VX and give a rational explanation for the absence of aging in crystallography and mass spectrometry experiments.

EXPERIMENTAL PROCEDURES

Caution

V-agents (VX, CVX, and VR) are highly toxic and are classified as a schedule 1 chemical as defined in the Chemical Weapons Convention. The handling of V-agents is dangerous and requires suitable personal protection, training, and facilities.

Chemicals

Racemic VX, *O*-ethyl-S-[2[bis(1-methyl-ethyl)amino] ethyl] methylphosphonothioate, VR, and CVX, were obtained from the Centre d'Étude du Bouchet-Maîtrise NRBC (Vert-le-Petit, France). Optically pure enantiomers of VX_R-(+) and VX_S-(−) were obtained from TNO (Rijswijk, The Netherlands). For the assignment of absolute configuration *R* or *S* of VX-(+/−), see Ref. 15.

Recombinant Human Butyrylcholinesterase

BChE was expressed in Chinese hamster ovary (CHO) cells and secreted into serum-free culture medium, and purified by affinity and ion-exchange chromatography as described earlier (16). The BChE enzyme was a truncated monomer containing residues 1–529 whose tetramerization domain was deleted.

Measurement of Inhibition Rate Constants for Pure Enantiomers of VX

BChE activities were assayed according to Ellman's method (17). BChE solution (17 nM final) was mixed with VX_S-(−) or VX_R-(+) (respectively, 21 and 88 nM final) in 100 mM phosphate buffer, pH 8.0. Each minute, 5 μl of the mixture was added to a well (96-well plate) filled with 100 μl of 0.8 mM 5,5′-dithiobis-(2-nitrobenzoic acid) in 100 mM phosphate buffer, pH 8.0. After the 7th aliquot (7 min), the wells were filled with 100 μl of 0.8 mM butyrylthiocholine in water. Absorbance was read at 412 nm immediately, then 5 min later. The net raise of absorbance is a direct measure of BChE activity. The initial concentration of VX_S-(−) is less than 2-fold the initial concentration of BChE which means that the inhibition follows second-order kinetics. The inhibition rate ki_S of BChE by VX_S-(−) was determined with the following equation,

$$\frac{1}{C - Ei} = \frac{1}{C} \cdot ki_S \cdot t \qquad \text{(Eq. 1)}$$

where C is the average concentration of enzyme and inhibitor (enzyme+inhibitor/2), Ei is the concentration of the inhibited enzyme, ki_S is the inhibition rate, and t is time.

The initial concentration of VX_R-(+) is more than 5 times the initial concentration of BChE which means that the inhibition follows pseudo-first-order kinetics. The inhibition rate ki_R of BChE by VX_R-(+) was determined with the following equation,

$$\log\frac{A_t}{A_0} = -\frac{ki_R \cdot I \cdot t}{2.303} \qquad \text{(Eq. 2)}$$

where A_t is the activity of human BChE at time t and A_0 at time 0, I is the initial concentration of VX_R-(+), ki_R is the inhibition rate, and t is time.

Crystals of V-agent-inhibited BChE Conjugates

BChE crystallized at a concentration of 8 mg/ml from 0.1 M MES, pH 6.5, supplemented with 2.1 M ammonium sulfate, using the hanging-drop system. The VX, CVX, and VR stock solutions were at 10 mM in 2-propyl alcohol. Crystals of conjugates were obtained using three different procedures.

Flash Soaking—Crystals of native BChE were flash-soaked into a solution containing 1 mM racemic V-agents or pure enantiomers VX for 5 min and flash-cooled in liquid nitrogen to prevent postinhibition reactions such as aging and/or spontaneous reactivation. Three soaking solutions were tested for racemic V-agents, from either 0.1 M MES, pH 6.5, or 0.1 M phosphate buffer, pH 7.4 or pH 8.0.

TABLE 1
X-ray data collection and refinement statistics

Enzyme	Racemate			Pure enantiomer	
	VX *in cristallo*	VR in solution	CVX in solution	VX_{S}-(−)	VX_{R}-(+)
PDB entry code	2XQF	2XQG	2XQI	2XQK	2XQJ
Data collection					
Space group	*I422*	*I422*	*I422*	*I422*	*I422*
Unit cell axes, $a = b$, c (Å)	155.1 128.1	154.6 127.6	155.2 127.0	154.9 127.4	155.8 128.3
X-ray source	ID14-eh4 (λ = 0.981)	ID14-eh1 (λ = 0.933)	ID14-eh2 (λ = 0.933)	ID23-eh1 (λ = 0.954)	
No. of reflections	409,037	249,879	223,406	214,798	284,598
Unique reflections	45,286	34,420	23,438	30,395	31,042
Resolution (Å)	48.0-2.1 (2.5-2.1)	41.5-2.3 (2.5-2.3)	49.1-2.6 (2.9-2.6)	41.5-2.4 (2.5-2.4)	49.3-2.4 (2.5-2.4)
Completeness (%)	99.2 (98.5)	99.7 (99.6)	96.0 (97.7)	99.5 (99.6)	99.9 (99.9)
R_{meas}[a] (%)	6.8 (30.8)	7.2 (48.8)	15.5 (50.4)	7.9 (48.9)	8.1 (41.5)
$I/\acute{o}$(I)	22.3 (7.9)	27.3 (4.8)	9.9 (4.1)	20.5 (5.3)	19.9 (6.2)
Redundancy	9.0 (8.7)	7.3 (7.4)	9.5 (9.0)	7.1 (6.9)	9.2 (9.7)
Refinement statistics					
R-factor[b] (R_{free})[c]	15.0 (18.9)	16.2 (21.4)	18.4 (24.7)	15.7 (21.7)	16.7 (22.3)
No. of atoms					
Protein	4269	4258	4258	4265	4246
Solvent	432	419	247	323	346
Others	193	185	186	183	161
Mean B-factor (Å^2)	37.1	38.1	54.0	41.2	39.7
Root mean square deviation from ideality					
Bond length (Å)	0.030	0.023	0.020	0.022	0.022
Angles (deg)	2.291	2.051	1.877	1.954	1.976
Chiral (Å^3)	0.207	0.144	0.127	0.136	0.139

[a] R_{meas} as defined in Ref. 31.
[b] R-factor = $\Sigma \mid F_o - \mid F_c \mid \mid / \Sigma \mid F_o \mid$, F_o, and F_c are observed and calculated structure factors.
[c] R_{free} set uses about 1000 of randomly chosen reflections.

Long Soaking—Crystals were long-soaked into a solution containing 1 mM racemic V-agents for 10 days to allow sufficient time for *in cristallo* aging.

Crystallization after Inhibition—Crystals were obtained from a solution of BChE first inhibited by 0.4 mM racemic V-agents in 5 mM MES, pH 6.5. In all three cases, the crystals were washed with a cryoprotectant solution (0.1 M MES, pH 6.5, with 2.3 M ammonium sulfate, containing 20% glycerol) and then flash-cooled in liquid nitrogen.

X-ray Data Collection and Structure of V-agent-BChE Conjugates

Diffraction data were collected at the European Synchrotron Radiation Facility (ESRF, Grenoble, France), at the ID29, ID23-1, ID14-1, ID14-2, and ID14-4 beam lines. All datasets were processed with XDS (18). The structures were solved by use of the CCP4 suite (19). An initial solution model was determined by molecular replacement, starting from the recombinant BChE structure (Protein Data Bank (PDB) entry 1P0I) from which all ligands (butyrate, glycerol, ions) and glycan chains were removed. For all diffraction data sets, the model was refined with REFMAC5 (20). An initial rigid body refinement was followed by iterative cycles of model building with Coot (21), and then restrained and TLS refinement was carried out with REFMAC5. The bound ligands and their descriptions were built using the Dundee PRODRG 2.5 server including energy minimization using GROMOS 96.1 force field.

Significant drops in R-factor and R_{free} occurred with TLS refinement. TLS groups were defined with the help of the TLS Motion Determination server (22). Refined TLS parameters are included in the deposited PDB file for each entry. Simulated annealing composite omit maps were calculated using Phenix (23) to check any bias in the model. Protein structures were illustrated using the program PyMOL.

RESULTS

Inhibition Rate Constants for Optically Pure VX Enantiomers—The bimolecular rate constant for the inhibition of recombinant BChE is $1.09 \pm 0.07 \times 10^7$ min^{-1} · M^{-1} ($n = 12$) for VX_S-(−) and $2.01 \pm 0.10 \times 10^6$ min^{-1} · M^{-1} ($n = 12$) for VX_R-(+). Thus, VX_S-(−) is only 5.4-fold more potent than VX_R-(+), in good agreement with literature data (12, 13).

X-ray Structure of Racemic V-agent-BChE Conjugates—We followed three different procedures to obtain the crystal structures of the conjugates. The flash-soaking procedure was aimed at obtaining the conjugate structure before any aging or spontaneous reactivation can take place. The long-soaking procedure intended to obtain the structure of the aged conjugate, and the procedure using inhibition in solution before crystallization was aimed at avoiding a possible enantioselectivity or aging bias introduced by the crystal packing. Still, we cannot exclude that a bias could persist during crystallization, if for example one enantiomeric conjugate crystallizes more favorably.

Whatever the procedure used, we systematically obtained identical conjugate structures with all three racemic V-agents, without any evidence for aging. The crystals belonged to the usual space group *I422*. The structures were refined at resolutions ranging from 2.1 to 2.6 Å. Data and refinement statistics for one dataset per V-agent are presented in Table 1. For each structure, a strong peak of electron density (>11σ) is observed in the $F_o - F_c$ map at covalent bonding distance of the catalytic serine Oγ, in agreement with the presence of the bound inhibitor. The oxygen of the phosphonate moiety is nested in the oxyanion hole, well stabilized by three hydrogen bonds with the main chain amide nitrogen of Gly-116, Gly-117, and Ala-199 (Fig. 1).

For all conjugates, the methyl group of the phosphonyl adducts points toward the catalytic histidine whereas the

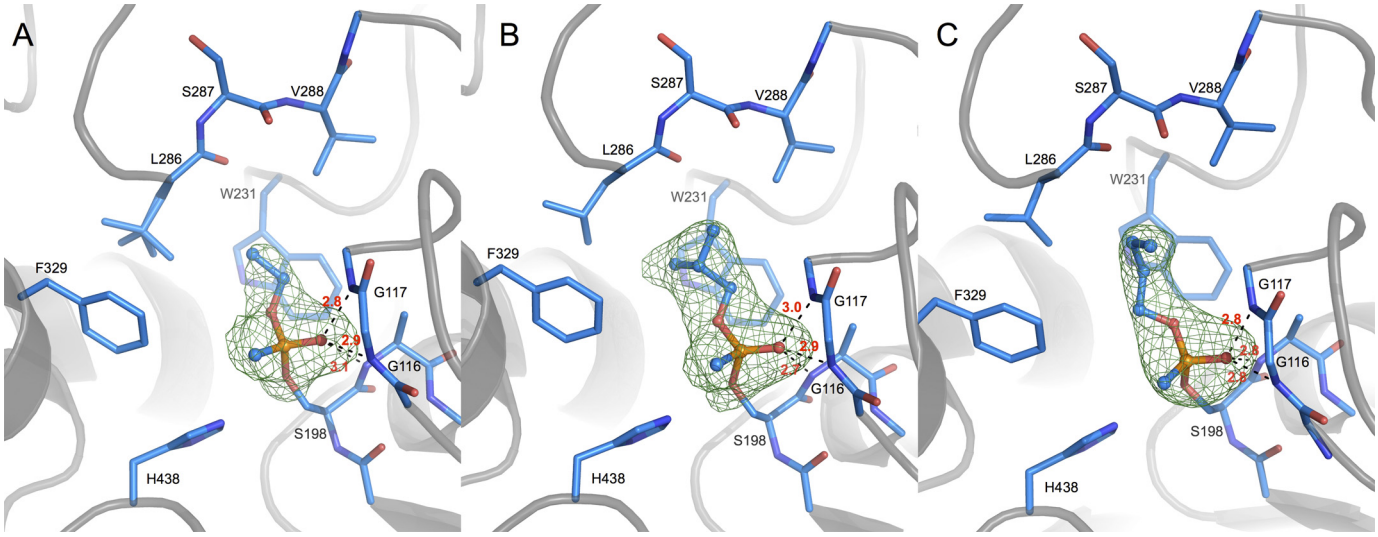

FIGURE 1. **Active site of VX-BChE (*A*), VR-BChE (*B*), and CVX-BChE (*C*) conjugates.** Crystals are obtained either by long soaking of BChE crystal in a 1 mM solution of racemic VX (*A*) or by crystallization of a solution containing 0.1 mM BChE inhibited by 0.4 mM of racemic VR (*B*) or CVX (*C*). Key residues are represented by *sticks* with carbon atoms in *blue*, oxygen atoms in *red*, nitrogen atoms in *dark blue*, and phosphorus atom in *orange*. Hydrogen bonds are represented by *black dashes*, and atomic distances are indicated in *red* (Å). Omit maps are represented in *green mesh*, contoured at 3.0 σ.

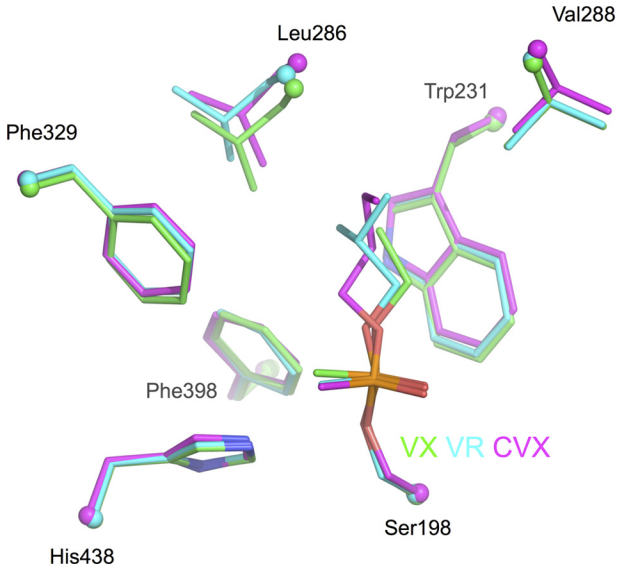

FIGURE 2. **Superimposition of the acyl-binding pocket region of VX-BChE (*cyan*), VR-BChE (*green*), and CVX-BChE (*magenta*) conjugates.** Key residues are represented by *sticks* with oxygen atoms in *red*, nitrogen atoms in *dark blue*, phosphorus atoms in *orange*. Cα atoms are represented as *spheres*.

alkoxy substituent is located in the acyl-binding pocket delimited by Trp-231, Leu-286, and Val-288 (Fig. 1). There is no doubt about the configuration assignment. The electron density maps show no evidence for the presence of the alternate configuration, *i.e.* the alkoxy group pointing toward the choline-binding pocket.

Adjustment of the acyl loop residues is observed, depending on the bulkiness of the alkoxy substituent (Fig. 2). Compared with the ethoxy substituent in the VX adduct, the isobutyloxy group of the VR adduct induces a 0.7 Å shift of Leu-286, and the *n*-butyloxy group of CVX adduct induces a 0.4-Å shift of Val-288 and 0.8-Å shift of Leu-286. Rearrangement of the acyl loop conformation was already observed for soman (24) and phosphoramidyl adducts (25). In addition, strain in the acyl-binding pocket translates into a slightly different position of the phosphonyl head for VX and CVX. The phosphorus atom shifts by 0.3 Å away from the pocket, and the phosphonyl moiety rotates about 20° around the SerOγ-P bond (Fig. 2). No other significant displacement of residues is observed compared with the native enzyme (PDB entry 1P0I).

Thus, the absolute configuration of the phosphorus atom for each adduct is P_S. The orientation of VX is identical to that observed in the recently solved structure of the VX-G117H mutant of BChE (PDB entry 2XMG) (26). This is the mirror image of the VX-*Tc*AChE adduct which is of configuration P_R: in this latter, the methyl substituent is located in the acyl-binding pocket, and the ethoxy group points toward the catalytic histidine inducing a conformational change (11).

The formation of the P_S adduct could result either from an in-line attack of VX_R-(+) with inversion of the phosphorus or an adjacent attack of VX_S-(−) and subsequent pseudorotation (27). In an effort to understand which VX enantiomer leads to the formation of the P_S adduct and what is the underlying mechanism, we solved the x-ray structure of BChE crystals flash-soaked in solutions containing pure enantiomers.

X-ray Structure of BChE Inhibited by Pure VX Enantiomers—The structures of VX_R-(+) and VX_S-(−) conjugates were solved to 2.4-Å resolution. Data and refinement statistics for one dataset per isomer are presented in Table 1.

The ethoxy substituent of VX_R-(+)-BChE conjugate is located in the acyl-binding pocket whereas the methyl points toward the catalytic histidine (Fig. 3*A*). The phosphorus atom is of absolute configuration P_S. This conformation is identical to that obtained by inhibition using a racemic mixture and in agreement with in-line phosphorylation (Scheme 2).

By contrast, the ethoxy substituent of VX_S-(−)-BChE points toward the catalytic histidine whereas the methyl group is located in the acyl-binding pocket (Fig. 3*B*). The phosphorus atom is of absolute configuration P_R, in agreement with in-line phosphorylation (Scheme 2). The two residues known to promote aging by dealkylation are close to the ethoxy group, His-

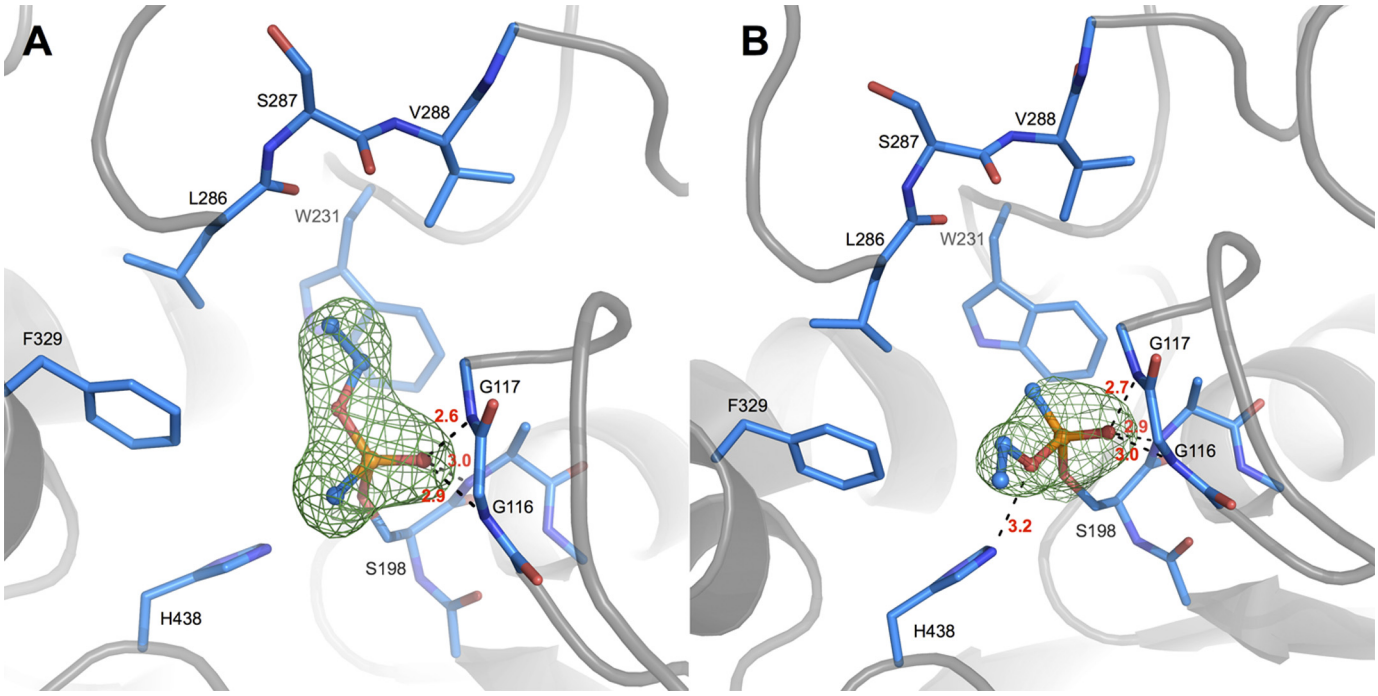

FIGURE 3. **Active site of VX_R-(+)-BChE (*A*) and VX_S-(−)-BChE (*B*) conjugates.** BChE crystals were flash-soaked in a 1 mM solution of VX_R-(+) (*A*) or VX_S-(−) (*B*). Key residues are represented by *sticks* with carbon atoms in *blue*, oxygen atoms in *red*, nitrogen atoms in *dark blue*, phosphorus atoms in *orange*. Hydrogen bonds are represented by *black dashes*, and atomic distances are indicated in *red* (Å). Omit maps are represented by a *green mesh*, contoured at 3.0 σ.

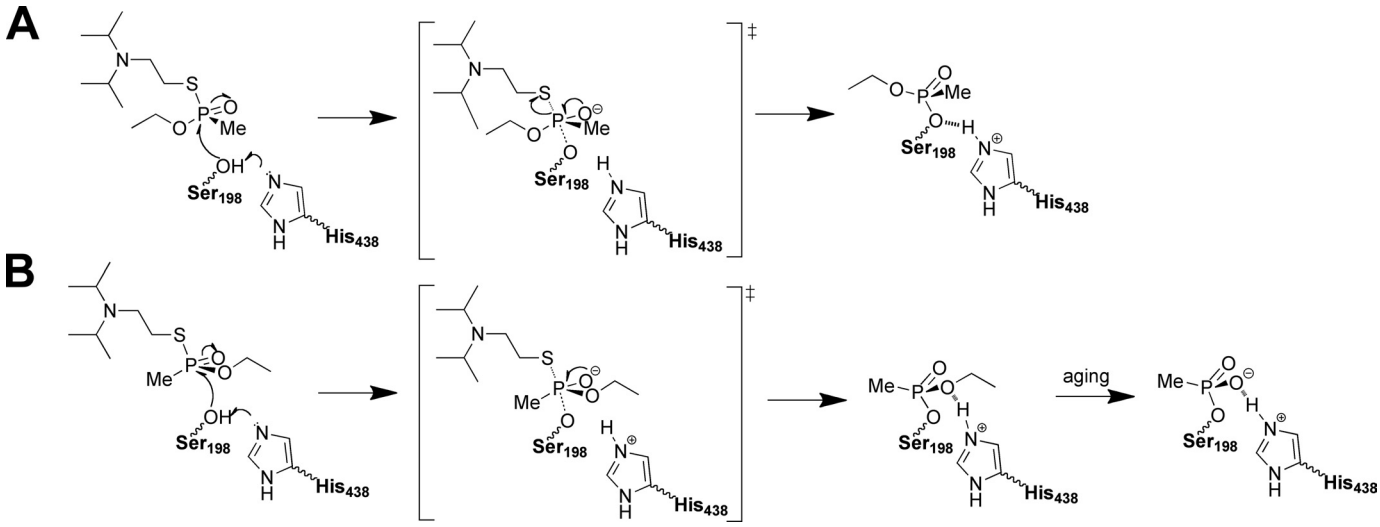

SCHEME 2. **Mechanism of inhibition of BChE by VX_R-(+) (*A*) and VX_S-(−) (*B*).**

438-Nϵ and the ethoxy oxygen being notably at H-bond distance (3.2 Å). This configuration is identical to that observed when *Tc*AChE was inhibited by racemic VX, except that no conformational change of the catalytic histidine is observed. The absence of conformational change of His-438 shows one more time that this catalytic residue is not mobile in BChE (25). These combined results suggest that in the presence of both enantiomers at submillimolar concentration, BChE will react preferentially with VX_R-(+).

DISCUSSION

We do not observe identical stereoselectivity for experiments performed in the presence of one or both enantiomers of V-agents. On the one hand, three different experiments using racemic VX, *i.e. in vivo* protection (14), mass spectrometry (10), and x-ray crystallography, show that BChE reacts preferentially with VX_R-(+) and does not age. On the other hand, kinetic experiments performed with separated VX_R-(+) or VX_S-(−) show a slight selectivity for VX_S-(−). Slow aging has been observed with VX_S-(−), $t_{1/2} \approx 50$ h, and no aging could be detected with VX_R-(+).[3] The absence of aging with VX_R-(+) is in agreement with the structural and mass spectrometry data. Noteworthy, very slow aging has been recently reported for BChE inhibited by racemic VX, $t_{1/2} = 77$ h (9). This half-time value seems to be intermediate between those of the VX_R-(+) and the VX_S-(−) conjugates.

[3] F. Worek, unpublished data.

There can be many different explanations for this discrepancy. A first hypothesis is that a shift in selectivity originates from the ability to bind multiple molecules at the same time in the active site gorge, especially at high concentrations. This is illustrated in the x-ray structure of aged soman-BChE conjugate in complex with butyrylthiocholine (24). Multiple binding affects the catalytic behavior of the enzyme. For example, at a high substrate concentration, binding of a second molecule of butyrylthiocholine in the active site gorge of BChE accelerates the turnover about three times (28). Thus, it is possible that in the presence of a racemic mixture, both enantiomers bind simultaneously in the active site gorge and interfere so that VX_R-(+) is in a position more favorable for the phosphonylation. This may be favored by the high concentrations of VX required for x-ray crystallography and mass spectrometry. Aging kinetic of BChE inhibited by racemic VX could provide some clues regarding this hypothesis, but the exact concentration of inhibitor was not reported (9). Although unexplained electron density is visible in the active site gorge of the conjugate, next to Trp-82, it does not correspond to a second molecule of V-agents in which P and S atoms large electron density is easily recognizable. An alternative hypothesis is that an unknown ligand corresponding to this unexplained electron density, often present in the choline-binding pocket of BChE (24–26), could alter the binding of VX_S-(−). Yet another hypothesis could be that even if both conjugates form in solution, the VX_R-(+)-BChE conjugate crystallizes more easily. In this case there would be a crystallization artifact for inhibited BChE. But this hypothesis also requires that there should be also a crystal packing artifact, VX_R-(+) binding more favorably to crystallized BChE. At this point we have no evidence to favor one of these nonmutually exclusive hypotheses.

Predicting the stereoselectivity of BChE for VR and CVX uniquely from the active site topology is not straightforward. The question is whether the large substituent of VR and CVX can fit in the acyl-binding pocket of BChE. Some clues were provided by structural data showing that a diethylamino group (TA1) or a *N*-propylamino group (TA6) do fit in that pocket (25). Here, the x-ray structures of VR- and CVX-BChE confirm that the long *n*-butyloxy of CVX or the bulky isobutyloxy of VR do fit as well. This explains why no aging was observed during mass spectrometry analysis of the VR-BChE conjugate or kinetics experiments (9). By extrapolation from VX, the P_S adducts results likely from the in-line attack by VR_R and CVX_R, whereas we expect a strong selectivity of human AChE for VR_S and CVX_S, knowing that VX_S-(−) is at least already 100-fold more reactive than VX_R-(+) (12, 13).

From a stereoselectivity point of view, hAChE appears as a better V-agents bioscavenger than hBChE. However, titration studies show that one equivalent of hAChE or hBChE is necessary to neutralize one equivalent of racemic VX in conditions simulating the estimated initial concentrations of VX during *in vivo* experiments (13). Actually, the phosphonylation rate of both VX enantiomers is higher than $10^6\ M^{-1} \cdot min^{-1}$ for both enzymes, so that the incubation time over 30 min was too long to discriminate their behavior. However, *in vivo* experiment shows that administration of hAChE gives a better survival rate of VX-exposed mouse (13).

Regarding the stereoselectivity of cholinesterases for G-agents tabun and soman, it has been established that human BChE and human AChE share the same selectivity (24, 29). Regarding sarin, bovine AChE reacts more than 4×10^3-fold faster with $sarin_S$-(−), the isopropyloxy substituent being too bulky for the AChE acyl-binding pocket, whereas the enantiomers inhibit horse serum BChE with virtually equal rates (30). Indeed, the structural data presented here and elsewhere show that the acyl-binding pocket of BChE can accommodate quite large substituents like isobutyloxy (VR) or diethylamino (TA1) (25). Moreover, mass spectrometry shows that the sarin-BChE conjugate does age by dealkylation, albeit partially (10). Aging by dealkylation suggests that the isopropyloxy substituent points toward His-438, *i.e.* the absolute configuration of the adduct is *R*, which in turn means that the enzyme reacted with $sarin_S$-(−). Incomplete aging could results either from insufficient reaction time or a significant portion of the enzyme inhibited by $sarin_R$-(+). In the latter case, both the kinetic experiment with horse serum BChE and the mass spectrometry analysis with human BChE show that these enzymes are not sufficiently enantioselective for sarin by contrast to AChE. This remains to be eventually supplemented by a structural study.

REFERENCES

1. Holmstedt, B. (1959) *Pharmacol. Rev.* **11,** 567–688
2. Silman, I., and Sussman, J. L. (2005) *Curr. Opin. Pharmacol.* **5,** 293–302
3. Li, B., Stribley, J. A., Ticu, A., Xie, W., Schopfer, L. M., Hammond, P., Brimijoin, S., Hinrichs, S. H., and Lockridge, O. (2000) *J. Neurochem.* **75,** 1320–1331
4. Saxena, A., Sun, W., Luo, C., Myers, T. M., Koplovitz, I., Lenz, D. E., and Doctor, B. P. (2006) *J. Mol. Neurosci.* **30,** 145–148
5. Masson, P., and Lockridge, O. (2010) *Arch. Biochem. Biophys.* **494,** 107–120
6. Lenz, D. E., Maxwell, D. M., Koplovitz, I., Clark, C. R., Capacio, B. R., Cerasoli, D. M., Federko, J. M., Luo, C., Saxena, A., Doctor, B. P., and Olson, C. (2005) *Chem. Biol. Interact.* **157–158,** 205–210
7. Ordentlich, A., Barak, D., Kronman, C., Benschop, H. P., De Jong, L. P., Ariel, N., Barak, R., Segall, Y., Velan, B., and Shafferman, A. (1999) *Biochemistry* **38,** 3055–3066
8. Masson, P., Nachon, F., and Lockridge, O. (2010) *Chem. Biol. Interact.* **187,** 157–162
9. Aurbek, N., Thiermann, H., Eyer, F., Eyer, P., and Worek, F. (2009) *Toxicology* **259,** 133–139
10. Li, H., Schopfer, L. M., Nachon, F., Froment, M. T., Masson, P., and Lockridge, O. (2007) *Toxicol. Sci.* **100,** 136–145
11. Millard, C. B., Koellner, G., Ordentlich, A., Shafferman, A., Silman, I., and Sussman, J. L. (1999) *J. Am. Chem. Soc.* **121,** 9883–9884
12. Reiter, G., Mikler, J., Hill, I., Weatherby, K., Thiermann, H., and Worek, F. (2008) *J. Chromatogr. B Analyt. Technol. Biomed. Life Sci.* **873,** 86–94
13. Cohen, O., Kronman, C., Raveh, L., Mazor, O., Ordentlich, A., and Shafferman, A. (2006) *Mol. Pharmacol.* **70,** 1121–1131
14. Kasten, S. A., Kajih, T., Smith, J. R., Oliver, Z., Otto, T. C., Reeves, T. E., Lenz, D. E., and Cerasoli, D. M. (2010) in *Proceedings of the 2010 Medical Defense Bioscience Review*, Hunt Valley, MD, May 24–27, 2010, p. 46, U.S. Army Medical Research and Development Command, Washington, DC
15. Hall, C. R., Inch, T. D., Inns, R. H., Muir, A. W., Sellers, D. J., and Smith, A. P. (1977) *J. Pharm. Pharmacol.* **29,** 574–576
16. Nachon, F., Nicolet, Y., Viguié, N., Masson, P., Fontecilla-Camps, J. C., and Lockridge, O. (2002) *Eur. J. Biochem.* **269,** 630–637
17. Ellman, G. L., Courtney, K. D., Andres, V., Jr., and Feather-Stone, R. M. (1961) *Biochem. Pharmacol.* **7,** 88–95
18. Kabsch, W. (2010) *Acta Crystallogr. D Biol. Crystallogr.* **66,** 125–132
19. Collaborative Computational Project 4 (1994) *Acta Crystallogr. D Biol.*

Crystallogr. **50,** 760–763
20. Murshudov, G. N., Vagin, A. A., and Dodson, E. J. (1997) *Acta Crystallogr. D Biol. Crystallogr.* **53,** 240–255
21. Emsley, P., and Cowtan, K. (2004) *Acta Crystallogr. D Biol. Crystallogr.* **60,** 2126–2132
22. Painter, J., and Merritt, E. A. (2006) *Acta Crystallogr. D Biol. Crystallogr.* **62,** 439–450
23. Adams, P. D., Grosse-Kunstleve, R. W., Hung, L. W., Ioerger, T. R., McCoy, A. J., Moriarty, N. W., Read, R. J., Sacchettini, J. C., Sauter, N. K., and Terwilliger, T. C. (2002) *Acta Crystallogr. D Biol. Crystallogr.* **58,** 1948–1954
24. Nicolet, Y., Lockridge, O., Masson, P., Fontecilla-Camps, J. C., and Nachon, F. (2003) *J. Biol. Chem.* **278,** 41141–41147
25. Carletti, E., Aurbek, N., Gillon, E., Loiodice, M., Nicolet, Y., Fontecilla-Camps, J. C., Masson, P., Thiermann, H., Nachon, F., and Worek, F. (2009) *Biochem. J.* **421,** 97–106
26. Nachon, F., Carletti, E., Wandhammer, M., Nicolet, Y., Schopfer, L. M., Masson, P., and Lockridge, O. (2011) *Biochem. J.* **434,** 73–82
27. Nachon, F., Carletti, E., Worek, F., and Masson, P. (2010) *Chem. Biol. Interact.* **187,** 44–48
28. Masson, P., Legrand, P., Bartels, C. F., Froment, M. T., Schopfer, L. M., and Lockridge, O. (1997) *Biochemistry* **36,** 2266–2277
29. Carletti, E., Colletier, J. P., Dupeux, F., Trovaslet, M., Masson, P., and Nachon, F. (2010) *J. Med. Chem.* **53,** 4002–4008
30. Boter, H. L., and van Dijk, C. (1969) *Biochem. Pharmacol.* **18,** 2403–2407
31. Diederichs, K., and Karplus, P. A. (1997) *Nat. Struct. Biol.* **4,** 269–275